

A Discrete-State Spiking Neuron Model and its Learning Potential

By

Hiroyuki TORIKAI*

Abstract

In this paper we review some of our recent results on discrete-state spiking neuron models. The discrete-state spiking neuron model is a wired system of shift registers and can generate various spike-trains by adjusting the pattern of the wirings. In this paper we show basic relations between the wiring pattern and characteristics of the spike-train. We also show a learning algorithm which utilizes successive changes of the wiring pattern. It is shown that the learning algorithm enables the neuron to approximate various spike-trains generated by a chaotic analog spiking neuron.

§ 1. Introduction

Various simplified spiking neuron models have been investigated from both fundamental and application viewpoints [1]-[17]. For example, integrate-and-fire models (including periodically driven ones) have been used to investigate spike-based information coding functions [3]-[26]. Also, the integrate-and-fire models have been used to construct pulse-coupled neural networks whose application potentials include image processing based on synchronization phenomena [7][6]. Inspired by such neuron models, we have proposed *discrete-state spiking neurons* (DSNs) [11]-[17] that can be regarded as discrete-state versions of simple analog neuron models as shown in Fig.1. The DSN can be implemented as a wired system of shift registers. We emphasize that the wiring pattern among the registers is a key parameter because the DSN can generate spike-trains having various *inter-spike intervals* (ISIs) by adjusting the wiring pattern. We have explored some fundamental questions on the DSN and have investigated approaches towards the questions as the followings.

Received February 27, 2009. Accepted May 26, 2009.

2000 Mathematics Subject Classification(s): 68Q80

*Graduate School of Engineering Science, Osaka University, Toyonaka, Osaka 560-8531, Japan.

e-mail: torikai@sys.es.osaka-u.ac.jp

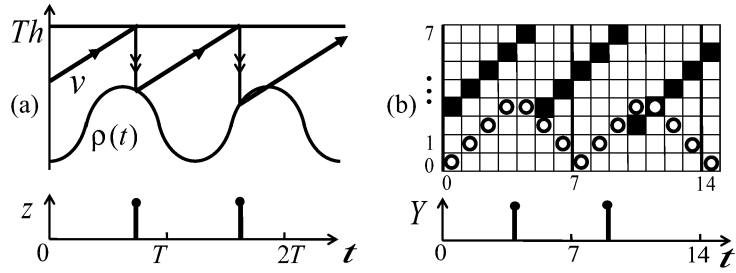


Figure 1. (a) Basic dynamics of integrate-and-fire neuron models in [2][8][10]. A potential v repeats *integrate-and-fire* dynamics between a threshold Th and a reset level $\rho(t)$. The periodic reset level $\rho(t)$ can realize rich bifurcation phenomena. $z(t)$ is an output spike-train. (b) Basic dynamics of the discrete-state spiking neuron [11]. The black box corresponds to the potential v and the white circle corresponds to the reset level $\rho(t)$. The black box repeats *shift-and-reset* dynamics that can be regarded as a discrete-state version of the integrate-and-fire dynamics. Y is an output spike-train.

- *Pulse coding*: What kind of information set can the DSN encode into spike-trains? We have analyzed basic characteristics of the spike-train and its symbolic dynamics [11][12].
- *Communication application*: Are the spike-trains of the DSN applicable to some engineering applications? We have clarified that the DSN can be applied to so-called ultra-wide band impulse radio technology [18] which utilizes spike-trains as spread spectrum codes [13][14].
- *Learning*: Can the DSN mimic unknown neuron dynamics? We have shown that the DSN can mimic another DSN with unknown parameter and an analog chaotic spiking neuron model by using a learning algorithm which utilizes successive changes of the wiring pattern [15]-[17].

In this paper we review some of our recent results on the last topic. First, we show basic relations between the wiring pattern and ISI characteristics. Some important results are summarized into a theorem. Second, based on the theorem, we show a learning algorithm. We then consider learning abilities of the DSN, where the DSN is used as a student and a chaotic analog spiking neuron [9] is used as a teacher. It is shown that, using the learning algorithm, the student can approximate various spike-trains generated by the analog teacher.

Significances of this paper are many, include the following points.

(a) Various discrete-state dynamical systems have been investigated from both fundamental and application viewpoints, e.g., cellular automaton and pseudo-random number generator [19]-[22]. Then our problem setting "synthesis of a spiking neuron model by discrete-state dynamics" *per se* would be an important fundamental problem. In addition, consideration of such a problem will contribute to develop a new discrete-state

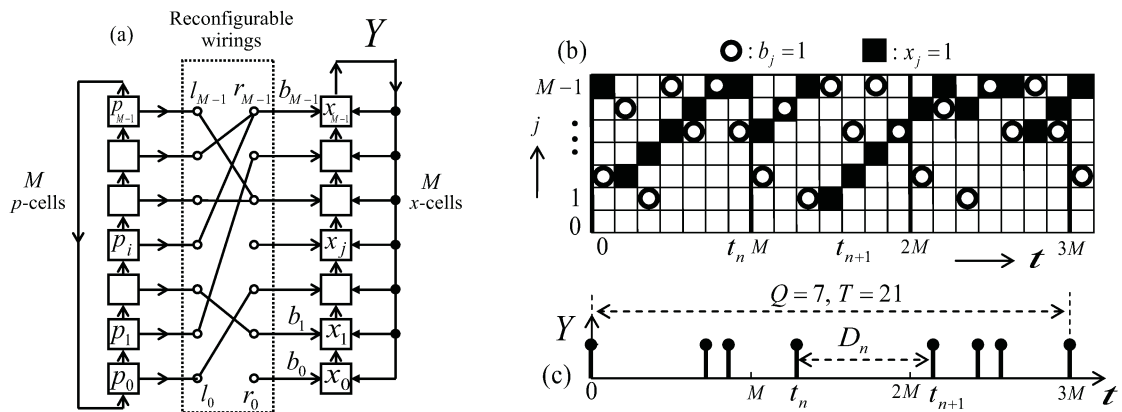


Figure 2. discrete-state spiking neuron (DSN). $M = 7$. (a) The DSN is a wired system of x -cells and p -cells that are shift registers. (b) The shift-and-reset dynamics. (c) Output spike-train Y .

dynamical system with bio-inspired learning and/or coupling mechanisms [5][23].

(b) The presented learning algorithm is based on change of the wiring pattern and thus it is suited for implementation based on reprogramming of a crossbar-switch on a field programmable gate array. On the other hand, if a learning algorithm utilizes change of analog parameter values, it is troublesome to implement the algorithm in an electronic circuit.

(c) We have investigated a simple pulse-coupled network of DSNs and its applications to spike-based information coding and multiplex communication [11]. We have also investigated application of the DSN to ultra-wide-band impulse-radio technology [13][14]. The results of this paper will contribute to develop learning methods for such digital pulse-coupled network and applications.

(d) The neural prosthesis (replacement of damaged biological neurons by artificial neurons, e.g., cochlea implant and brain implant) is a recent hot topic [24]-[27]. In order to develop the neural prosthesis, a fundamental problem is construction of an artificial neuron model that can mimic biological neurons. Hence the results of this paper will be fundamentals to develop the neural prosthesis in the future.

§ 2. Discrete-State Spiking Neuron

In this section we introduce the *discrete-state spiking neuron* (DSN) and explain its basic dynamics [11]. The DSN operates on a discrete time $t = 0, 1, 2, \dots$. As shown in Fig.2(a), the DSN has M pieces of p -cells that are indexed by $i \in \{0, 1, \dots, M-1\}$, where $M \geq 2$. Each p -cell has a digital state $p_i(t) \in \mathbf{B} := \{0, 1\}$. The p -cells are

ring-coupled and are governed by

$$(2.1) \quad \begin{aligned} p_i(t+1) &= p_{i-1}(t) \quad \text{for } 1 \leq i \leq M-1, \\ p_0(t+1) &= p_{M-1}(t). \end{aligned}$$

In this paper initial states of the p -cells are fixed to $p_0(0) = 1$ and $p_k(0) = 0$ for all $k \neq 0$. Then the p -cells oscillate periodically with period M . As shown in Fig.2(a), the DSN has one-way reconfigurable wirings from the left terminals (l_0, \dots, l_{M-1}) to the right terminals (r_0, \dots, r_{M-1}) . The left terminals accept a state vector $\mathbf{P}(t) := (p_0(t), \dots, p_{M-1}(t))^t \in \mathbf{B}^M$ of the p -cells. Each left terminal l_i has one wiring, and each right terminal r_j can accept any number of wirings. In order to describe pattern of the wirings, let us introduce an $M \times M$ *wiring matrix* \mathbf{A} whose element is defined by $a(j, i) = 1$ if the left terminal l_i is wired to the right terminal r_j ; and $a(j, i) = 0$ otherwise. The DSN in Fig.2(a) has the following wiring matrix.

$$(2.2) \quad \mathbf{A} = \begin{pmatrix} 0 & 0 & 0 & 0 & 0 & 0 & 0 & 0 \\ 0 & 0 & 1 & 0 & 0 & 0 & 0 & 0 \\ 1 & 0 & 0 & 0 & 0 & 0 & 0 & 0 \\ 0 & 0 & 0 & 0 & 0 & 0 & 0 & 0 \\ 0 & 0 & 0 & 0 & 1 & 0 & 1 & 0 \\ 0 & 1 & 0 & 0 & 0 & 0 & 0 & 0 \\ 0 & 0 & 0 & 1 & 0 & 1 & 0 & 1 \end{pmatrix}.$$

The wiring matrix \mathbf{A} has one "1" in each column. The right terminals (r_0, \dots, r_{M-1}) output a *base signal* $\mathbf{b}(t) := (b_0(t), \dots, b_{M-1}(t))^t \in \mathbf{B}^M$ which can be described by

$$(2.3) \quad \mathbf{b}(t) = \mathbf{A}\mathbf{P}(t).$$

In Fig.2(b), white circles represent a base signal $\mathbf{b}(t)$ which corresponds to the wiring pattern in Fig.2(a). Here let us consider the x -cells. Each j -th x -cell has a digital state $x_j(t) \in \mathbf{B}$. Also, as shown in Fig.2(a), the x -cell has three digital inputs $\{b_j, x_{M-1}, x_{j-1}\}$, where $x_{-1} := 0$. The x -cell operates as follows: $x_j(t+1) = x_{j-1}(t)$ if $x_{M-1}(t) = 0$, and $x_j(t+1) = b_j(t)$ if $x_{M-1}(t) = 1$. Let $(x_0(t), \dots, x_{M-1}(t))^t := \mathbf{X}(t) \in \mathbf{B}^M$ be a state vector of the x -cells, and let $S((x_0, \dots, x_{M-1})^t) = (0, x_0, \dots, x_{M-2})^t$ be a shift operator. Then dynamics of the x -cells is described by

$$(2.4) \quad \mathbf{X}(t+1) = \begin{cases} S(\mathbf{X}(t)) & \text{if } x_{M-1}(t) = 0, \quad (\text{Shift}) \\ \mathbf{b}(t) & \text{if } x_{M-1}(t) = 1. \quad (\text{Reset}) \end{cases}$$

Basic dynamics of the x -cells is shown in Fig.2(b). A black box at (t, j) represents that the x -cell has state $x_j(t) = 1$. If the black box is below the highest position which is indexed by $j = M-1$, the black box is shifted upward. If the black box reaches the highest position at $t = t_n$ (i.e., $x_{M-1}(t_n) = 1$), the black box at $t = t_n + 1$ is reset to

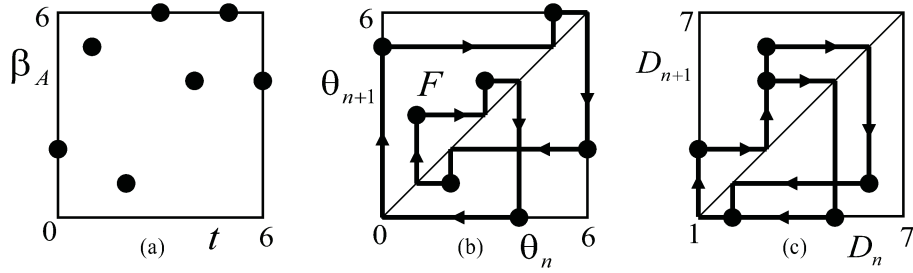


Figure 3. Maps corresponding to the DSN in Fig.2. (a) Base index function β_A . (b) Phase map F . The initial condition is $\theta_1 = 0$ and the phase map F generates the sequence $(\theta_1, \theta_2, \dots, \theta_7) = (0, 5, 6, 2, 1, 3, 4)$. (c) Sequence $(D_1, D_2, \dots, D_7) = (5, 1, 3, 6, 2, 1, 3)$ of ISIs on the (D_n, D_{n+1}) -plane.

the position of the white circle at $t = t_n$. At this reset moment, the DSN outputs a spike $x_{M-1}(t_n) = 1$. Repeating such *shift-and-reset* dynamics, the DSN oscillates. Let

$$(2.5) \quad Y := \{x_{M-1}(0), x_{M-1}(1), x_{M-1}(2), \dots\}$$

and call Y a *spike-train*. As a result, the dynamics of the DSN is described by Equations (2.1), (2.3), (2.4) and (2.5). Also the DSN is characterized by the following parameters: number M of p -cells; number M of x -cells; and elements $a(j, i)$ of $M \times M$ wiring matrix \mathbf{A} . Relations between the parameters (M, \mathbf{A}) and characteristics of the spike-train Y is studied in the next section.

§ 3. Various Spike-Trains and Problem Statement

In this section we show that the DSN can generate various spike-trains Y by adjusting the parameters (M, \mathbf{A}) . Let us begin with defining *inter-spike interval* (ISI) and its periodicity (see also Fig.2(c)).

Definition: An integer $t \in \mathbf{Z}_{\geq 0} = \{0, 1, 2, \dots\}$ is the spike position $\stackrel{\text{def}}{\Leftrightarrow} x_{M-1}(t) = 1$.

Let us denote the spike positions by $t_0 = 0 < t_1 < \dots$ in increasing order and call t_n the n -th spike position. Let $D_n = t_{n+1} - t_n$ and call it the n -th ISI. A spike-train Y is *periodic* if there exists a positive integer Q such that $t_{n+Q} \equiv t_n \pmod{M}$ for all $n \geq 1$. In this case the minimum integer Q such that $t_{n+Q} \equiv t_n \pmod{M}$ is said to be *ISI number* of the periodic spike-train Y . A sequence $\mathbf{D} := (D_1, D_2, \dots, D_Q)$ is said to be *ISI sequence* of the periodic spike-train Y . $T := \sum_{n=1}^Q D_n$ is said to be *period* of the periodic spike-train Y .

The spike-train Y in Fig.2(c) can be characterized by

$$(3.1) \quad \begin{aligned} \text{ISI number } Q &= 7, \\ \text{ISI sequence } \mathbf{D} &= (5, 1, 3, 6, 2, 1, 3). \end{aligned}$$

In order to consider time evolution of spike position t_n (i.e., dynamics of t_n), let us define a *base index function* $\beta_A : \mathbf{Z}_{\geq 0} \rightarrow \mathbf{Z}_M := \{0, 1, \dots, M-1\}$, $t \mapsto \beta_A(t)$, which satisfies

$$a(\beta_A(t), t) = 1$$

where t is treated as modulo M . Fig.3(a) shows the base index function $\beta_A(t)$ corresponding to the DSN in Fig.2. As shown in these figures, the base index function $\beta_A(t)$ can be regarded as a time-waveform of the base signal $\mathbf{b}(t)$. Let us define the n -th *spike phase* θ_n by

$$\theta_n = t_n \pmod{M}$$

where $\theta_n \in \mathbf{Z}_M$. Then we obtain the following proposition.

Proposition:

$$(3.2) \quad \theta_{n+1} = F(\theta_n) := \theta_n + M - \beta_A(\theta_n) \pmod{M}, \quad F : \mathbf{Z}_M \rightarrow \mathbf{Z}_M.$$

Proof of this proposition can be found in [15]. We refer to F as the *phase map*. In addition, the ISI D_n is given by a function of the spike position t_n as follows.

$$D_n = M - \beta_A(\theta_n).$$

Fig.3(b) and (c) show the phase map F and a sequence of ISI D_n on the (D_n, D_{n+1}) -plane that correspond to the DSN in Fig.2. In these figures, the initial condition is $\theta_1 = 0$, and the sequences $(\theta_1, \theta_2, \dots, \theta_7) = (0, 5, 6, 2, 1, 3, 4)$ and $(D_1, D_2, \dots, D_7) = (5, 1, 3, 6, 2, 1, 3)$ are obtained. We can clarify basic relations between parameters (M, \mathbf{A}) and characteristics of the output spike-train Y as follows.

- The possible longest ISI is determined by the number M of x -cells, i.e., $1 \leq D_n \leq M$.
- The possible maximum ISI number is determined by the number M of p -cells, i.e., $1 \leq Q \leq M$. This is because the domain \mathbf{Z}_M of the phase map F has M elements.
- Various shapes of the phase map F (i.e., rich dynamics of the phase θ_n) can be realized by adjusting the wiring matrix \mathbf{A} . This is because various shapes of the base index function $\beta_A(t)$ can be realized by adjusting the wiring matrix \mathbf{A} .

In the next section we consider an approach toward the question.

Based on such richness of the spike phase dynamics, in this paper we consider the problem statement depicted in Fig.4. The *teacher spike-train* \tilde{Y} is a given spike-train which has a *teacher ISI sequence* $\tilde{\mathbf{D}} = (\tilde{D}_1, \dots, \tilde{D}_{\tilde{Q}})$, where the tilde " ~ " represents "teacher" hereafter. The teacher ISI sequence $\tilde{\mathbf{D}}$ is input to a *student DSN*. The student DSN generates a *student spike-train* Y which has a *student ISI sequence* $\mathbf{D} = (D_1, \dots, D_Q)$. Now we have the following fundamental question.

Can the student DSN reproduce or approximate the teacher ISI sequence $\tilde{\mathbf{D}}$ by using a learning algorithm which utilizes successive changes of the wiring matrix \mathbf{A} ?

§ 4. Basic theorem and learning algorithm

In this section we give a basic theorem and define a distance between ISI sequences. Using the theorem and the distance, we present a learning algorithm and demonstrate its abilities by illustrative examples.

§ 4.1. Re-Wiring Theorem

Let us consider change of a wiring matrix \mathbf{A}^{old} into a different wiring matrix \mathbf{A}^{new} . We refer to such change of wiring matrix as *re-wiring*. The superscripts "old" and "new" represent "*original version*" and "*re-wired version*," respectively, hereafter. As an example of \mathbf{A}^{old} , let us use the $M \times M$ wiring matrix \mathbf{A} in Equation (2.2). First, the wiring matrix \mathbf{A}^{old} whose element is denoted by $a^{old}(j, i)$ is transformed into an $M \times M$ matrix \mathbf{H}^{old} whose element $h^{old}(j, i)$ is defined by

$$(4.1) \quad h^{old}(j, i) = \begin{cases} a^{old}(i - j, i) & \text{for } j \leq i, \\ a^{old}(i - j + M, i) & \text{for } j > i. \end{cases}$$

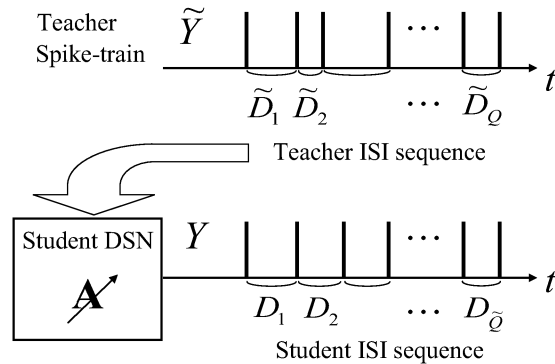


Figure 4. A problem setting: can the student DSN reproduce or approximate the teacher ISI sequence $\tilde{\mathbf{D}} = (\tilde{D}_1, \dots, \tilde{D}_{\tilde{Q}})$ by using a learning algorithm which is based on successive changes of the wiring matrix \mathbf{A} ?

The wiring matrix $\mathbf{A}^{old} = \mathbf{A}$ in Equation (2.2) is transformed into

$$(4.2) \quad \mathbf{H}^{old} = \begin{pmatrix} 0000100 \\ 0010000 \\ 0000001 \\ 0100000 \\ 0001000 \\ 1000000 \\ 0000010 \end{pmatrix}.$$

This matrix \mathbf{H}^{old} can be regarded as *transition matrix representation* of the phase map F in Fig.3(b). Hence we refer to \mathbf{H}^{old} as *transition matrix*. Second, the transition matrix \mathbf{H}^{old} is changed into a different transition matrix \mathbf{H}^{new} by swapping the r -th and the s -th rows, and then swapping the r -th and the s -th columns. We refer to the integers (r, s) as *re-wiring positions*. As an example, let us use $(r, s) = (5, 6)$. Then the transition matrix \mathbf{H}^{old} in Equation (4.2) is changed into

$$(4.3) \quad \mathbf{H}^{new} = \begin{pmatrix} 0000100 \\ 0010000 \\ 0000010 \\ 0100000 \\ 0001000 \\ 0000001 \\ 1000000 \end{pmatrix}.$$

Finally, the transition matrix \mathbf{H}^{new} whose element is denoted by $h^{new}(j, i)$ is transformed into a an $M \times M$ wiring matrix \mathbf{A}^{new} whose element $a^{new}(j, i)$ is defined by

$$(4.4) \quad a^{new}(j, i) = \begin{cases} h^{new}(i - j, i) & \text{for } j \leq i, \\ h^{new}(i - j + M, i) & \text{for } j > i. \end{cases}$$

The matrix \mathbf{H}^{new} in Equation (4.3) is transformed into

$$(4.5) \quad \mathbf{A}^{new} = \begin{pmatrix} 0000000 \\ 1010001 \\ 0000000 \\ 0000010 \\ 0000100 \\ 0100000 \\ 0001000 \end{pmatrix}.$$

Fig.5(a) shows the DSN with the re-wired matrix \mathbf{A}^{new} in Equation (4.5). We note that a re-wiring leads to change of at most four wirings of the DSN. In the case of Fig.5(a), the three bold wiring are different from the wirings in Fig.2(a). Fig.5(b) shows the phase map F^{new} of the re-wired DSN. Let us explain how the phase map is changed by the re-wiring. We denote a *transposition* of $m \in \mathbf{Z}_M$ and $n \in \mathbf{Z}_M$ by $\sigma_{m,n}(\theta)$, i.e.,

$$(4.6) \quad \sigma_{m,n}(m) = n, \quad \sigma_{m,n}(n) = m \quad \text{and} \quad \sigma_{m,n}(\theta) = \theta \quad \text{for } \theta \neq m, n.$$

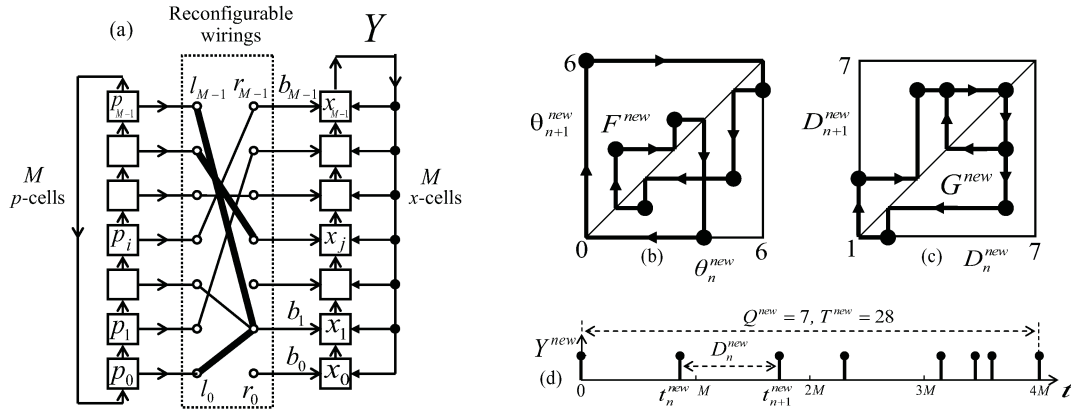


Figure 5. Re-wired DSN. (a) The bold wirings are difference from the wirings in Fig.2(a). (b) Phase map F^{new} . (c) Sequence of ISI D_n on the $(D_n^{new}, D_{n+1}^{new})$ -plane. (d) Output spike-train Y^{new} whose ISI sequence is difference from the ISI sequence in Fig.2(c).

Then, for given re-wiring positions (r, s) , we have a relation $F^{new} = \sigma_{r,s} \circ F \circ \sigma_{r,s}$. Actually, by comparing Fig.3(b) and Fig.5(b), we can confirm $F^{new} = \sigma_{5,6} \circ F \circ \sigma_{5,6}$. Fig.5(c) shows a sequence of ISI D_n on the (D_n, D_{n+1}) -plane generated by the re-wired DSN. Fig.5(d) shows the spike-train Y^{new} which is characterized by

$$(4.7) \quad \begin{aligned} & \text{ISI number } Q^{new} = 7, \\ & \text{ISI sequence } \mathbf{D}^{new} = (6, 6, 4, 6, 2, 1, 3). \end{aligned}$$

Comparing Equations (4.7) and (3.1), we can see that the ISI number is invariant ($Q^{new} = Q$) but the ISI sequence is changed ($\mathbf{D}^{new} \neq \mathbf{D}$) by the re-wiring. In the following, we give some generalized results. We assume that the re-wiring positions satisfy $1 \leq r < s \leq M - 1$. We then introduce the following.

Re-wiring rule: A wiring matrix \mathbf{A}^{old} is transformed into a transition matrix \mathbf{H}^{old} via Equation (4.1). The transition matrix \mathbf{H}^{old} is changed into a transition matrix \mathbf{H}^{new} by swapping the r -th and the s -th rows, and then swapping the r -th and the s -th columns. The transition matrix \mathbf{H}^{new} is transformed into the re-wired matrix \mathbf{A}^{new} via Equation (4.4).

We assume that the initial states $x_j^{old}(0)$ and $x_j^{new}(0)$ of the original and the re-wired DSNs are fixed to

$$(4.8) \quad \begin{aligned} & x_{M-1}^{old}(0) = x_{M-1}^{new}(0) = 1, \\ & x_k^{old}(0) = x_k^{new}(0) = 0 \text{ for } k \neq M - 1. \end{aligned}$$

This initial state setting guarantees that the 1-st spike positions of the original DSN and the re-wired DSN are to be $t_1^{old} = 0$ and $t_1^{new} = 0$, respectively. Then we obtain

the following theorem.

Theorem: Let a DSN have a wiring matrix \mathbf{A}^{old} and let it generate a periodic spike-train with ISI number Q^{old} . Then, for arbitrary re-wiring positions (r, s) , the re-wired DSN generates a periodic spike-train with ISI number $Q^{new} = Q^{old}$. That is, the ISI number is invariant under the re-wiring rule.

Proof of this theorem can be found in [15]. By comparing Equations (3.1) and (4.7), we can confirm the theorem. A role of the theorem in a learning is discussed in section 5.

§ 4.2. Distance of ISI sequences

Let a teacher ISI sequence $\tilde{\mathbf{D}}$ and a student ISI sequence \mathbf{D}^{old} have the same ISI number \tilde{Q} . We then define a distance between $\tilde{\mathbf{D}}$ and \mathbf{D}^{old} as follows.

$$(4.9) \quad C(\tilde{\mathbf{D}}, \mathbf{D}^{old}) = \frac{1}{\tilde{T}} \sum_{n=1}^{\tilde{Q}} |\tilde{D}_n - D_n^{old}|, \quad \tilde{T} = \sum_{n=1}^{\tilde{Q}} \tilde{D}_n.$$

That is, C is a Manhattan distance between $\tilde{\mathbf{D}}$ and \mathbf{D}^{old} normalized by period \tilde{T} of the teacher spike-train \tilde{Y} . For example ISI sequences $\tilde{\mathbf{D}} = (1, 2, 3)$ and $\mathbf{D}^{old} = (3, 2, 1)$ have distance $C = (|1 - 3| + |2 - 2| + |3 - 1|)/(1 + 2 + 3) = 4/6$. The distance C measures degree of differences between the ISI sequences $\tilde{\mathbf{D}}$ and \mathbf{D}^{old} as follows.

- $C(\tilde{\mathbf{D}}, \mathbf{D}^{old}) = 0$ implies $\tilde{\mathbf{D}} = \mathbf{D}^{old}$. In this case the student DSN reproduces the teacher ISI sequence $\tilde{\mathbf{D}}$.
- $C(\tilde{\mathbf{D}}, \mathbf{D}^{old}) > 0$ implies $\tilde{\mathbf{D}} \neq \mathbf{D}^{old}$. In this case the student DSN approximates the teacher ISI sequence $\tilde{\mathbf{D}}$ with distance C . A smaller distance C means a smaller approximation error.

§ 4.3. Learning Algorithm

Using the distance C and the re-wiring rule, we present the following learning algorithm whose flow-chart is in Fig.6.

Step 1. Initialization: Initialize the wiring matrix \mathbf{A}^{old} as

$$(4.10) \quad a^{old}(j, i) := \begin{cases} 1 & \text{for } j = M - 1 \text{ and } i \neq \tilde{Q} - 1, \\ 1 & \text{for } j = Q - 1 \text{ and } i = \tilde{Q} - 1, \\ 0 & \text{otherwise.} \end{cases}$$

for all i and j , where " := " denotes "substitution of the right side into the left side" hereafter. Initialize a counter k for iteration number to $k := 0$.

Step 2. Re-wiring: Generate random integers (r, s) such that $1 \leq r < s \leq M - 1$.

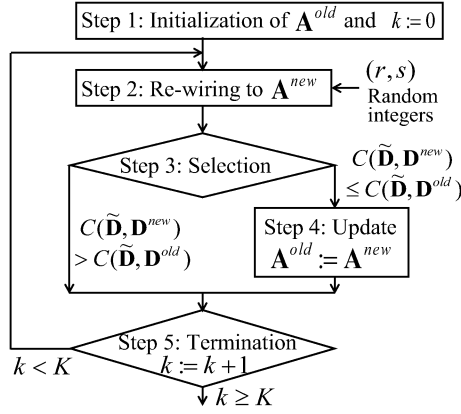


Figure 6. Learning algorithm.

Applying the re-wiring rule with the re-wiring positions (r, s) to \mathbf{A}^{old} , create a re-wired matrix \mathbf{A}^{new} .

Step 3. Selection: If $C(\tilde{\mathbf{D}}, \mathbf{D}^{new}) \leq C(\tilde{\mathbf{D}}, \mathbf{D}^{old})$ then go to step 4. If $C(\tilde{\mathbf{D}}, \mathbf{D}^{new}) > C(\tilde{\mathbf{D}}, \mathbf{D}^{old})$ then go to step 5. That is, the distance C is used as a cost function.

Step 4. Update: Update the wiring matrix as $\mathbf{A}^{old} := \mathbf{A}^{new}$.

Step 5. Termination: Let K be a given maximum iteration number. Increment the counter k by one. If $k < K$, then go to step 2. If $k \geq K$, then terminate the algorithm.

In order to explore abilities of the learning algorithm, let us consider the following example.

§ 4.4. Example: Approximation of analog chaotic neuron

As an example, let us study a problem setting where the teacher spike-train \tilde{Y} is generated by an analog neuron model. As an example, let us use a chaotic *analog spiking neuron* (ASN) that can be regarded as a two-dimensional version of the integrate-and-fire neuron [9]. The dynamics of the ASN is described by

$$\frac{d}{d\tau} \begin{bmatrix} x \\ y \end{bmatrix} = \begin{bmatrix} \delta & 1 \\ -1 & \delta \end{bmatrix} \begin{bmatrix} x \\ y \end{bmatrix} \quad \text{for } x < 1,$$

$$(x(\tau^+), y(\tau^+)) = (\mu, y(\tau) - \lambda(1 - \mu)) \text{ if } x(\tau) = 1,$$

$$(4.11) \quad z(\tau) = \begin{cases} 0 & \text{for } x(\tau) < 1, \\ 1 & \text{if } x(\tau) = 1 \end{cases}$$

where τ is a continuous time, τ^+ denotes $\lim_{\epsilon \rightarrow 0} \tau + \epsilon$, x and y are analog states, and z is an output. The ASN is characterized by the analog parameters (λ, μ, δ) . Basic

dynamics of the ASN is shown in Fig.7. If $x < 1$, the state x vibrates as shown in Fig.7(a) and the trajectory of (x, y) rotates around the origin $(0, 0)$ as shown in Fig.7(b). If $x = 1$, the states (x, y) are reset to $(\mu, y - \lambda(1 - \mu))$ and a spike $z = 1$ is generated as shown in Fig.7(a). In the parameter case of Fig.7(b), the ASN generates a periodic spike-train $z(\tau)$ whose ISIs $\{s_n\}$ have real number values. In a steady state, we sample q ISIs $\mathbf{s} := (s_1, \dots, s_q)$, where the number of samples $q = 10$ is commonly used in this paper. The ISI sequence \mathbf{s} in Fig.7(b) can be integerized into an ISI sequence $\tilde{\mathbf{D}} = (4, 6, 4, 6, 4, 6, 4, 6, 4, 6)$ with ISI number $\tilde{Q} = 2$. This ISI sequence $\tilde{\mathbf{D}}$ is used as a teacher ISI sequence. Fig.8(a) shows a teacher spike-train \tilde{Y} represented by this teacher ISI sequence $\tilde{\mathbf{D}}$. As a student, a DSN with system size $M = q$ is used. Fig.8(b) shows the student spike-trains Y^{old} just after the initialization in step 1. By the initialization, the ISI number Q^{old} of the student spike-train Y^{old} is to be identical with the ISI number $\tilde{Q} = 2$ of the teacher spike-train \tilde{Y} . The theorem guarantees that the ISI number Q^{old} is invariant during the learning. Fig.8(c) and (d) show the student spike-trains Y^{old} after $k = 10$ and $k = 50$ learning iterations, respectively. In the case of Fig.8(d), the student DSN reproduces the teacher ISI sequence $\tilde{\mathbf{D}}$. Fig.9 shows characteristics of the distance C . We can see that the DSN can approximate the teacher ISI sequence $\tilde{\mathbf{D}}$ within distance $C \simeq 0.01$ in average after about $k = 150$ learning iterations, and can reproduce $\tilde{\mathbf{D}}$ in some learning trials.

Now, let us consider the case where the ASN generates a chaotic spike-train. In the parameter case of Fig.10, the ASN generates a chaotic spike-train $z(\tau)$ whose ISIs $\{s_n\}$ have real number values. In a steady state, we sample $q = 10$ ISIs $\mathbf{s} := (s_1, \dots, s_q)$. The ISI sequence \mathbf{s} in Fig.10 can be integerized into an ISI sequence $\tilde{\mathbf{D}} = (3, 6, 8, 3, 8, 1, 3, 7, 2, 9)$. This ISI sequence $\tilde{\mathbf{D}}$ is used as a teacher ISI sequence. Fig.11(a) shows a teacher spike-train \tilde{Y} which is represented by this teacher ISI sequence $\tilde{\mathbf{D}}$. As a student, a DSN with system size $M = q$ is used. The student accepts the ISI sequence $\tilde{\mathbf{D}}$ as an input and obeys the learning algorithm. Fig.11(b)-(d) show student spike-trains Y^{old} in a learning trial. We can confirm that the student ISI sequence \mathbf{D}^{old} approaches to the teacher ISI sequence $\tilde{\mathbf{D}}$ as the learning proceeds. In the case of Fig.11(d), the student DSN approximates the teacher ISI sequence $\tilde{\mathbf{D}}$ with the distance $C = 6/50$. Fig.12 shows characteristics of the distance C . We can see that the DSN can approximate the teacher ISI sequence $\tilde{\mathbf{D}}$ within distance $C \simeq 0.15$ in average after about $k = 500$ learning iterations. Note that, from a mathematical viewpoint, the DSN with an arbitrary system size M (including $M \rightarrow \infty$) can be investigated. From a VLSI implementation view point, however, the system size M (number of shift registers) is limited. Now we are analyzing relations between learning performances (e.g., convergence speed, number of local minima and their attraction domains, approximation error, VLSI power consumption) for the system size M .

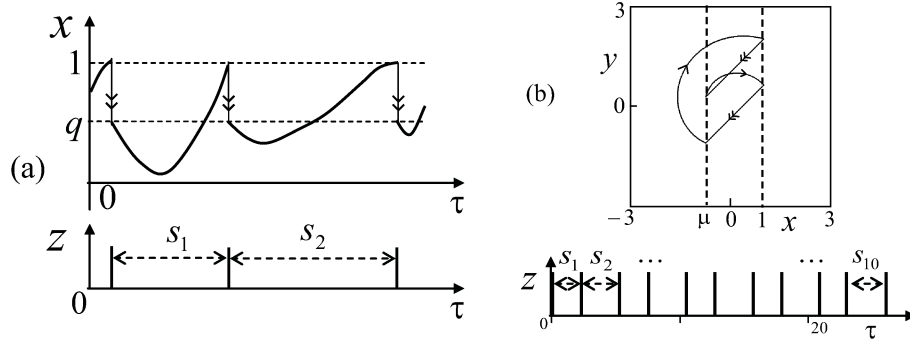


Figure 7. Analog spiking neuron [9]. (a) Basic dynamics. (b) Periodic attractor and periodic spike-train $z(\tau)$. $\delta = 0.18$, $\lambda = 1.0$ and $\mu = -0.75$.

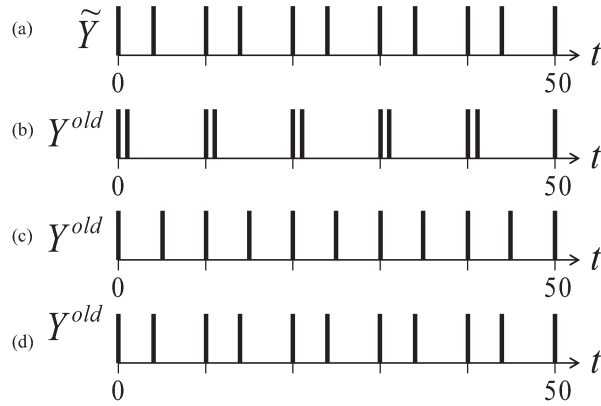


Figure 8. A learning trial. (a) Teacher spike-train \tilde{Y} whose ISI sequence $\tilde{D} = (4, 6, 4, 6, 4, 6, 4, 6, 4, 6)$ is given by integerizing the periodic ISI sequence s in Fig.7(b). (b)-(d) Student spike-trains Y^{old} . (b) After initialization. $D^{old} = (1, 9, 1, 9, 1, 9, 1, 9, 1, 9)$ and $C = 30/50$. (c) After $k = 10$ learning iterations. $D^{old} = (5, 5, 5, 5, 5, 5, 5, 5, 5, 5)$ and $C = 10/50$. (d) After $k = 50$ learning iterations. $D^{old} = \tilde{D}$ and $C = 0$. The student DSN reproduces the teacher ISI sequence \tilde{D} .

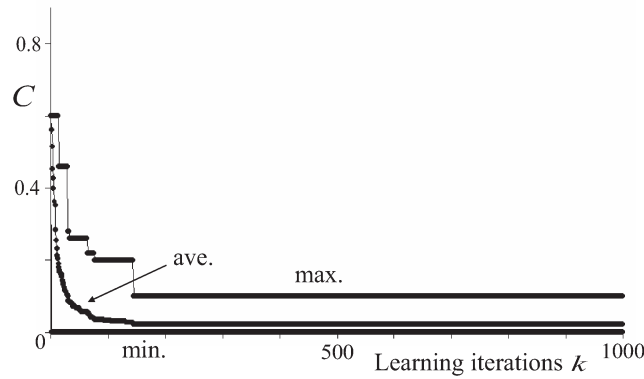


Figure 9. Characteristics of the distance C for 40 learning trials. $M = q = 10$. The teacher ISI sequence \tilde{D} is the integerized periodic ISI sequence in Fig.8.

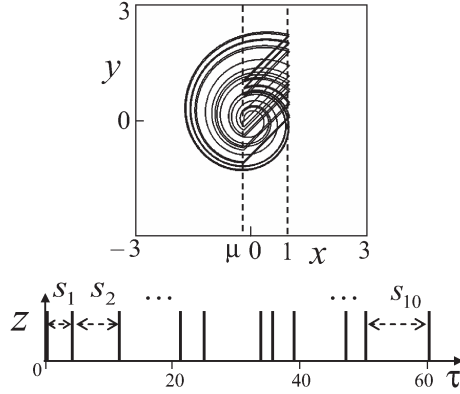


Figure 10. Chaotic attractor and chaotic spike-train $z(\tau)$ of the analog spiking neuron. $\delta = 0.18$, $\lambda = 1.0$ and $\mu = -0.18$.

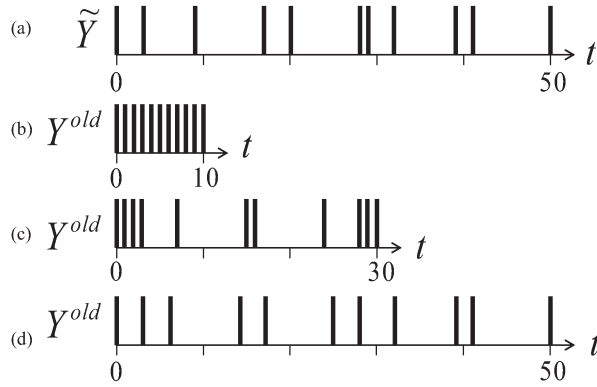


Figure 11. A learning trial. (a) Teacher spike-train \tilde{Y} whose ISI sequence $\tilde{D} = (3, 6, 8, 3, 8, 1, 3, 7, 2, 9)$ is given by integerizing the samples chaotic ISI sequence \mathbf{s} in Fig.10. (b)-(d) Student spike-trains Y^{old} in a learning trial. (b) After initialization. $D^{old} = (1, 1, 1, 1, 1, 1, 1, 1, 1, 1)$ and $C = 40/50$. (c) After 1 learning iteration. $D^{old} = (1, 1, 1, 4, 8, 1, 4, 8, 1, 1)$ and $C = 32/50$. (d) After 150 learning iterations. $D^{old} = (3, 3, 8, 3, 8, 3, 4, 7, 2, 9)$ and $C = 6/50$.

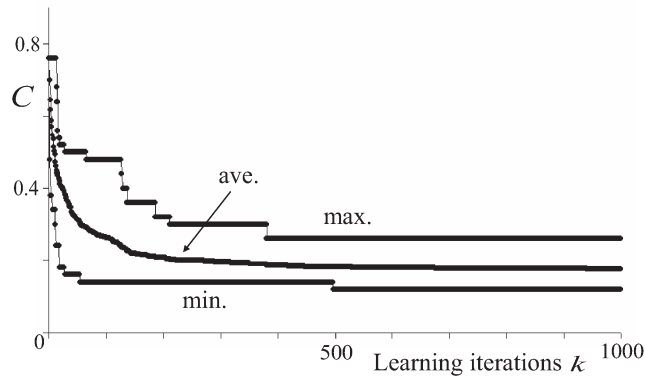


Figure 12. Characteristics of the distance C for 40 learning trials. $M = q = 10$. The teacher ISI sequence \tilde{D} is the integerized and sampled chaotic ISI sequence in Fig.10.

§ 5. Conclusions

We have introduced the DSN which is a wired system of shift registers. We have shown basic relations between the pattern of the wirings and characteristics of the spike-train. We have also introduced the learning algorithm which utilizes successive changes of the wiring pattern. We have shown that the DSN can approximate various spike-trains from the analog spiking neuron.

Let us consider the case where the ISI number of a teacher spike-train is $\tilde{Q} = M$. In this case the number of all the wiring matrixes of the student DSN is M^M . If the learning algorithm randomly creates a re-wired matrix without obeying the theorem, the search space of the learning is the set of M^M wiring matrixes. In these M^M wiring matrixes, however, there exist only $(M - 1)!$ wiring matrixes that lead to ISI number M of the student spike-trains. The significance of the theorem is that it can restrict the search space from the M^M wiring matrixes into the $(M - 1)!$ wiring matrixes.

Future problems include the followings. (a) Analysis of the learning performances. (b) Clarification of class of neuron models (and biological neurons) that can be mimicked by the DSN. (c) Application of the DSN to neural prosthesis, e.g., cochlea implant and brain implant [24]-[27].

References

- [1] Izhikevich, E.M. (2006). Dynamical systems in neuroscience, MIT Press.
- [2] Perez, R & L Glass, L. (1982). Bistability, period doubling bifurcations and chaos in a periodically forced oscillator, Phys. Lett. vol.90A, no.9, pp.441-443.
- [3] Lindner, B., Chacron, M.J. & Longtin, A. (2005). Integrate-and-fire neurons with threshold noise: A tractable model of how interspike interval correlations affect neuronal signal transmission, Physical Review E 72, 021911.
- [4] Hamanaka, H., Torikai, H. & Saito, T. (2006). Quantized spiking neuron with A/D conversion functions, IEEE Trans. Circuits Syst. II, 53, 10, pp. 1049-1053.
- [5] R. Eckhorn, Neural mechanisms of scene segmentation: recordings from the visual cortex suggest basic circuits for linking field models, IEEE Trans. Neural Networks, vol.10, no.3, pp.464-479, 1999.
- [6] J. J. Hopfield & A. V. M. Herz, Rapid local synchronization of action potentials: Toward computation with coupled integrate-and-fire neurons, Proc. Natl. Acad. Sci. USA, vol. 92, pp. 6655-6662, 1995.
- [7] S. R. Campbell, D. Wang & C. Jayaprakash, Synchrony and desynchrony in integrate-and-fire oscillators, Neural computation, vol. 11, pp. 1595-1619, 1999.
- [8] G. Lee & N. H. Farhat, The bifurcating neuron network 2, Neural networks, vol.15, pp.69-84, 2002.
- [9] H. Nakano & T. Saito, Grouping synchronization in a pulse-coupled network of chaotic spiking oscillators, IEEE Trans. Neural Networks, 15, 5, pp. 1018-1026, 2004.
- [10] H. Torikai & T. Saito, Synchronization phenomena in pulse-coupled networks driven by spike-train inputs, IEEE Trans. Neural Networks, vol. 15, no. 2, pp.337-347, 2004.

- [11] H. Torikai, H. Hamanaka & T. Saito, Reconfigurable Digital Spiking Neuron and its Pulse-Coupled Network: Basic Characteristics and Potential Applications, *IEEE Trans. CAS-II*, vol.53, no.8, pp. 734-738, 2006.
- [12] H. Torikai, Basic Spike-train properties of a Digital Spiking Neuron, *Journal of American Institute of Mathematical Sciences - Discrete and Continuous Dynamical Systems Series B*, 9, 1, pp.183-198, 2008.
- [13] H. Torikai, Basic Characteristics and Learning Potential of a Digital Spiking Neuron, *IEICE Trans. Fundamentals*, Vol.E90-A No.10 pp.2093-2100, 2007.
- [14] Akira Hirata and Hiroyuki Torikai, Learning of Digital Spiking Neurons for Ultra Wide Band Applications, *Proc. ICCNS*, p. 124, 2008.
- [15] H. Torikai, A. Funew and T. Saito, Digital spiking neuron and its learning for approximation of various spike-trains, *Neural Networks*, 21, 2-3, pp. 140-149, 2008.
- [16] Hiroyuki Torikai and Sho Hashimoto, A Hardware-oriented Learning Algorithm for a Digital Spiking Neuron, *Proc. IEEE-INNS/IJCNN*, pp. 2472-2479, 2009.
- [17] Sho Hashimoto and Hiroyuki Torikai, A Novel Hybrid Spiking Neuron: response analysis and learning potential, *Proc. ICONIP*, 2008 (accepted).
- [18] M-G. Di Benedetto and G. Giancola, *Understanding Ultra Wide Band Radio Fundamentals*, Prentice Hall, 2004.
- [19] S. Wolfram, Universality and complexity in cellular automata, *Pysica D*, vol. 10, pp. 1-35, 1984.
- [20] L. O. Chua, S. Yoon & R. Dogaru, A nonlinear dynamics perspective of Wolfram's new kind of science. Part I: threshold of complexity, *Int. J. Bif. and Chaos*, vol. 12, no.12, pp.2655-2766, 2002.
- [21] C. S. Hsu, & R. S. Guttalu, A Universal Algorithm for Global Analysis of Dynamical Systems: An Application of Cell-to-Cell Mappings, *Trans. ASME*, vol.47, pp.940-948, 1980.
- [22] D. E. Knuth, *The art of computer programming*, vol.2, 3rd edn., Addison Wesley, 1998.
- [23] G. Bi & M. Poo, Synaptic modifications in cultured hippocampal neurons: Dependence on spike timing, synaptic strength, and postsynaptic cell type, *J. Neurosci.*, vol.18, pp. 10464-10472, 1998.
- [24] C. D. Geisler, *From sound to synapse: physiology of the mammalian ear*, Oxford University Press, 1998.
- [25] Martignoli, S., van der Vyver, J.-J., Kern, A., Uwate, Y., Stoop, R. (2007). Analog electronic cochlea with mammalian hearing characteristics, *Applied Physics Letters*, 91, 064108.
- [26] Hiroyuki Torikai and Toru Nishigami, A novel artificial model of spiral ganglion cell and its spike-based encoding function, *Proc. ICONIP* (2008) (accepted)
- [27] T. W. Berger and D. L. Glangzman, *Toward replacement parts for the brain - Implantable biomimetic electronics as neural prosthesis*, The MIT Press, 2005.